

Microscopic mass formulas

J. Duflo¹ and A.P. Zuker²

¹Centre de Spectrométrie Nucléaire et de Spectrométrie de Masse (IN2P3-CNRS), 91405 Orsay Campus, France

²Physique Théorique, Bât40/1 CRN, IN2P3-CNRS/Université Louis Pasteur BP 28, F-67037 Strasbourg Cedex 2, France

(Received 3 March 1994; revised manuscript received 13 April 1995)

By assuming the existence of a pseudopotential smooth enough to do Hartree-Fock variations and good enough to describe nuclear structure, we construct mass formulas that rely on general scaling arguments and on a schematic reading of shell model calculations. Fits to 1751 known binding energies for $N, Z \geq 8$ lead to rms errors of 375 keV with 28 parameters. Tests of the extrapolation properties are passed successfully. The Bethe-Weizsäcker formula is shown to be the asymptotic limit of the present one(s). The surface energy of nuclear matter turns out to be probably smaller than currently accepted.

PACS number(s): 21.10.Dr, 21.60.-n

The local structure of the mass surfaces [1] is fairly smooth and amenable to algebraic analyses of shell model origin [2,3] that lead to precise mass formulas—the rms errors may go below 400 keV [4]—but they need many parameters and have questionable extrapolation properties far from stability. The droplet (FRDM) [5] and Thomas-Fermi (EFTSI) [6] mass tables are designed to reach the neutron drip-line, as demanded by calculations of r -process nucleosynthesis, but they are not very precise: with 30 parameters the former yields an rms error of 673 keV for $N, Z \geq 8$ while the latter needs only 9 parameters for an rms error of 730 keV for $A \geq 36$.

In a recent fit [7] it was shown that with 12 parameters the rms error for $N \geq 28$, $Z \geq 20$ could go down to 385 keV. This fit does not extrapolate well and assumes *a priori* knowledge of the right closures and the right boundaries between spherical and deformed regions. In a companion paper [8] rigorous microscopic guidelines were proposed to take advantage of the simplicity detected in [7], while eliminating the drawbacks. A brief review of these guidelines will make clear which is the problem to be solved to obtain a good mass formula.

The starting point is a basic separation property of the interaction (anticipated in [9] but proven in [8]): A (renormalized) Hamiltonian, *ready for use in a shell model calculation*, can be written as $H = H_m + H_M$.

The monopole part,

$$H_m = \sum_{k,l} a_{kl} m_k (m_l - \delta_{kl}) + b_{kl} \left(T_k \cdot T_l - \frac{3m_k}{4} \delta_{kl} \right), \quad (1)$$

contains only quadratic forms in the number (m_k) and isospin (T_k) operators for orbits k . The expectation value of H_m for any state is the average energy of the configuration to which it belongs (a configuration is a set of states with fixed m and T for each orbit). In particular H_m reproduces the exact energy of closed shells and single particle (or hole) states built on them, since for this set (which we call $cs \pm 1$) each configuration contains a single member. We have emphasized the fact that Eq. (1) is ready for shell model calculations because its form is not the usual one, in which effective core and single particle terms are separated from the two-body parts acting in the valence space. It should be

noted that the kinetic energy can always be written as two body by eliminating the center-of-mass contribution.

The multipole Hamiltonian H_M contains all other terms (pairing, quadrupole, etc.), and does not affect the $cs \pm 1$ states that bound the shell model spaces.

This general result depends only on the assumption that there exists a pseudopotential smooth enough to do Hartree-Fock (HF) variation. The renormalization process that defines the effective interaction leads also to many body forces that vanish at the closed shells. Their effects cannot be distinguished from those of the other higher rank terms that will appear later in simulating configuration mixing [8].

In [9] it was shown that H_M is well given by the realistic nucleon-nucleon interactions, and therefore parameter-free while H_m must be treated phenomenologically because of the poor saturation properties of these forces. The problem is that Eq. (1) contains hundreds of parameters, each of them a function of A and T ($T = |N - Z|/2$). In the context of [9] local fits are possible because only a fraction of the parameters are active and information on the $cs \pm 1$ states is available. To say something general about H_m and, in particular, to construct a mass table, we must proceed differently.

We shall find how to extract from Eq. (1) the few dominant terms responsible for bulk properties and shell formation. We show how to mock configuration mixing through simple algebraic expressions, and how to determine the spherical-deformed boundaries. The results of a fit and its asymptotic behavior are discussed.

To discover the form of the dominant terms in H_m we rely on two geometric properties of the realistic forces.

(1) *The A, T dependence.* The a_{kl} and b_{kl} coefficients in Eq. (1) must behave as typical matrix elements

$$V(\omega)_{klmn} \cong \frac{\omega}{\omega_0} V(\omega_0)_{klmn} + O(\omega^2), \quad (2)$$

a result from Ref. [9], but adding an $O(\omega^2)$ correction warranted for large oscillator constant ω . Then we know that

$$\hbar \omega = \frac{34.6A^{1/3}}{\langle r^2 \rangle} \cong 40A^{-1/3}, \quad (3)$$

a classical result [10] obtained with the standard $\langle r^2 \rangle = 0.86A^{2/3}$. A much better fit to the radii is obtained with $\langle r^2 \rangle = 0.90R_c^2$ where $R_c = A^{1/3}[1 - (T/A)^2]$ [7].

By combining this result with Eqs. (2) and (3), and calling a typical term in Eq. (1) $\hat{\Gamma}(A, T)$, we obtain

$$\Gamma(A, T) = (\Gamma/R)[1 - \rho(\Gamma)/R], \quad R = R_c^2/A^{1/3} \quad (4)$$

for the amplitude $\Gamma(A, T)$ affecting operator $\hat{\Gamma}$. (The caret symbol will be omitted when no confusion is possible.)

(2) *Diagonal form. The isoscalar master terms.* The matrices a_{kl} and b_{kl} in Eq. (1) can be reduced to diagonal form. For a_{kl} , say, we have

$$\sum_{k,l} a_{kl} m_k m_l = \sum_{\mu} e_{\mu} \left(\sum_k m_k f_{k_{\mu}} \right)^2 \quad (5)$$

and we borrow from [11] the result that the largest contribution (by far) to a realistic force has the form

$$\hat{\Gamma}_0 \Gamma_0(A) = \left(\sum_p m_p / \sqrt{D_p} \right)^2 e_0, \quad (6)$$

where m_p is the number operator for the oscillator shell of principal quantum number p , and D_p is the degeneracy [$D_p = (p+1)(p+2)$]. Calling $M = \sum m_p / \sqrt{D_p}$, setting $m_p = n_p + z_p$, where n, z are number operators for neutrons (ν) and protons (π), and filling shells p_{ν} and p_{π} up to some $p_{f\nu}$ and $p_{f\pi}$ Fermi level, we find

$$\langle M \rangle \cong \frac{1}{2} [(3N)^{2/3} + (3Z)^{2/3}] = O(A^{2/3}) \quad (7)$$

where we have approximated $\sqrt{(p+1)(p+2)} \approx p + 3/2$, and used $N = \sum n_{p_{\nu}} = \sum (p_{\nu} + 1)(p_{\nu} + 2) \cong \frac{1}{3}(p_{f\nu} + 2)^3$ and $Z = \frac{1}{3}(p_{f\pi} + 2)^3$.

Therefore $\langle \hat{\Gamma}_0 \rangle = O(A^{4/3})$, and, from Eq. (4) we have $\langle \hat{\Gamma}_0 \rangle \Gamma(A, T) = O(A)$. As we shall see, this term is responsible for most of the bulk energy. At the same time it produces strong magicity at the harmonic oscillator (HO) closures through the $\sqrt{D_p}$ scaling of the m_p operators. This effect is absent in an infinite medium, where $a_{kl} = O(A^{-1})$ and the total number operator $m = \sum m_p$ replaces the eigenvector M to ensure the $O(A)$ behavior of the energy.

If M is viewed as a coherent state, by symmetry the other eigenvectors that can be constructed out of m_p operators are simply these same operators orthogonalized to M . Then we expect another monopole term of the form $P = \sum f(p) m_p^2 / D_p$, which goes either as $A^{2/3}$ if $f(p) = O(1)$, or as A if $f(p) = O(p)$.

By now we can state the general rule: *Monopole terms must be symmetric quadratic forms of properly scaled operators.*

Proper scaling is determined by the assumed form of the amplitudes [i.e., Eq. (4)], and by the asymptotic properties expected (or postulated) for each term. It is worth pointing out that proper scaling is a delicate matter that must be decided on empirical grounds, and to illustrate the possible ambiguities we consider a particular a_{kl} coefficient in Eq. (1) and take k and l to belong to the same major shell. As a

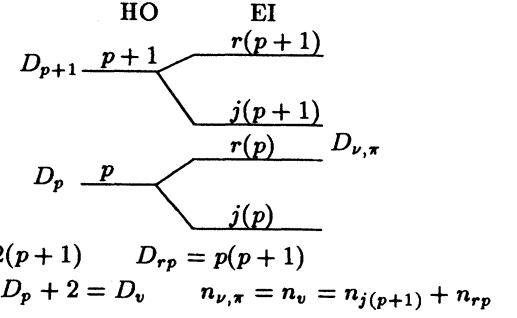


FIG. 1. HO and EI major shells.

contributor to the main term M^2 [i.e., Eq. (6)] a_{kl} must contain a part that goes as $\omega/D_p = O(A^{-1})$, but it also contains a contribution to $P = \sum f(p) m_p^2 / D_p$, which goes as $f(p)\omega/D_p$, i.e., $O(A^{-1})$ if $f(p) = O(1)$, or $O(A^{-2/3})$ if $f(p) = O(p)$. Hence, a_{kl} may go either as A^{-1} , or as a sum of $O(A^{-1})$ and $O(A^{-2/3})$ terms. In Ref. [12], an $A^{-0.75}$ scaling is extracted from experimental spectra, favoring the latter option, i.e., $f(p) = O(p)$.

Spin-orbit and isovector terms. In deciding which are the contributions that are necessarily present beyond the ones already discovered, we consider eigenvectors orthogonal to M . To obtain the observed extruder-intruder closures (EI) we need spin-orbit (SO) effects and we introduce

$$S_p = p m_{jp} - 2 m_{rp} = (\tilde{l} \cdot \tilde{s})_p. \quad (8)$$

Here (refer to Fig. 1) jp is the largest orbit in the p th shell and rp regroups all the others. $(\tilde{l} \cdot \tilde{s})_p$ is the operator that produces the same splittings as $(l \cdot s)_p$ and then collapses the r -orbits to their centroid value. The rationale for considering only two types of orbits is clear from Fig. 1: we want to give top priority to shell formation (i.e., the cs part of the $cs \pm 1$ set). The combinations of m_k operators other than m_j and m_r will contribute to subshell effects that we incorporate in H_M and treat later. It should be noted the formation of the EI closures is not inconsistent with the survival of HO ones in the light nuclei.

The other necessary ingredients are the isovector counterparts of m_p and s_p . Calling

$$t_p = |n_p - z_p|,$$

$$S_p = p(n_{jp} + z_{jp}) - 2(n_{rp} + z_{rp}),$$

and

$$S_{t_p} = p|n_{jp} - z_{jp}| - 2|n_{rp} - z_{rp}|,$$

we introduce the variables

$$MA_p = \frac{m_p}{\sqrt{D_p}}, \quad SA_p = \frac{S_p}{2(p+1)}, \quad (9a)$$

$$MT_p = \frac{t_p}{\sqrt{D_p}}, \quad ST_p = \frac{S_{t_p}}{2(p+1)}. \quad (9b)$$

TABLE I. The operators $\hat{\Gamma}$ (called Γ here) in H_m , H_s , and H_d .

H_m	$\alpha=1/2$	$R_c=A^{1/3}(1-(T/A)^2)$
$FMA=(\Sigma MA_p)^2$	$FSA=(\Sigma SA_p)^2$	$FCA=\Sigma MA_p D_p^{-1/2} \Sigma SA_p D_p^{-1/2}$
$PMA=\Sigma(MA_p)^2 D_p^\alpha$	$PSA=\Sigma(SA_p)^2 D_p^\alpha$	$PCA=\Sigma(MA_p)(SA_p) D_p^{\alpha-1}$
$FMT=(\Sigma MT_p)^2$	$FST=(\Sigma ST_p)^2$	$FCT=\Sigma MT_p D_p^{-1/2} \Sigma ST_p D_p^{-1/2}$
$PMT=\Sigma(MT_p)^2 D_p^\alpha$	$PST=\Sigma(ST_p)^2 D_p^\alpha$	$PCT=\Sigma(MT_p)(ST_p) D_p^{\alpha-1}$
$4T(T+1)A^{-2/3}$	$V_p=-\text{mod}(N,2)-\text{mod}(Z,2)$	$V_c=[-Z(Z-1)+0.76[Z(Z-1)]^{2/3}]/R_c$
$H_s \quad (\bar{n}=D_\nu-n, \quad \bar{z}=D_\pi-z)$	$S2=n\bar{n}D_\nu^{-1}+z\bar{z}D_\pi^{-1}$	$S3=n\bar{n}(n-\bar{n})D_\nu^{2(\beta-1)}+z\bar{z}(z-\bar{z})D_\pi^{2(\beta-1)}$
$SQ+=2(n\bar{n})^2 D_\nu^{2\beta-3}+2(z\bar{z})^2 D_\pi^{2\beta-3}$	$SQ-=4n\bar{n}z\bar{z}(D_\nu D_\pi)^{\beta-3/2}$	$\beta=1/2$
$H_d \quad (n'=n-JU, \bar{n}'=\bar{n}+JU),$	$(z'=z-JU, \bar{z}'=\bar{z}+JU)$	$D3=n'\bar{n}'(n'-\bar{n}')D_\nu^{-2}+z'\bar{z}'(z'-\bar{z}')D_\pi^{-2}$
$QQ_1^0=(n'\bar{n}'D_\nu^{-3/2}\pm z'\bar{z}'D_\pi^{-3/2})^2$	$QQ\pm=QQ0\pm QQ1$	$D0=16JU=4$

Finally we construct the 12 possible symmetric quadratics shown in the first part of Table I]. The abbreviations are (F=full, P=partial), (M=master, S=SO, C=cross), (A=isoscalar, T=isovector). The C terms are hybrids that could not represent eigensolutions in Eq. (5), but they could modify (i.e., mix) slightly the M and S terms. They have been introduced to ensure—through FCA and FCT—the presence of representatives of the conventional spin-orbit force, including possible isospin effects. It is only for “symmetry” reasons in Table I that PCA and PCT are also present, but their effects are not expected to be significant and they will be excluded from the fits considered in this paper.

FSA and FCA are scaled as the ordinary $\zeta l \cdot s$ term with $\zeta=O(A^{-2/3})$ [10]. The FXT operators are scaled as the FXA ones ($X=M, S, \text{ or } C$). For the PXY contributions ($Y=A$ or T) we introduce a factor D_p^α to allow for possible ambiguities in the $f(p)$ factor discussed above. The fits will decide in favor of $\alpha=1/2$.

In addition to these terms, H_m includes pairing (V_p) and Coulomb (V_c) contributions as well as a $4T(T+1)$ term whose presence we explain below. Although V_p belongs in principle with H_M , it has been incorporated here because it affects equally all nuclei. Similarly V_c contains multipole parts, but at the level of precision we work they are negligible.

Asymptotic form of the master terms. Except for a small contribution from PMA and PMT (when $\alpha=1/2$), the asymptotic expressions

$$FMA \approx \left(\frac{3}{2}A\right)^{4/3} \left[1 - \frac{2}{9}(2T/A)^2\right]$$

and

$$FMT \approx \left(\frac{3}{2}A\right)^{4/3} \left(\frac{4T}{3A}\right)^2$$

determine the bulk and symmetry energies of nuclear matter. As these quantities must emerge from a balance of potential and kinetic energies that our arguments have bypassed, the shell effects produced by FMA and FMT may be partially spurious and it is convenient to decouple them from the asymptotic contributions by adding these as independent terms.

The three operators that turn out to be favored by the fits are $4T(T+1)/A^{2/3}$, and FM+ and PM+ where $XM+=XMA+XMT$ ($X=F, P$), whose asymptotic form is

$$XM+=1.717A^{4/3}+0.3816(2T)^2/A^{2/3}+O(A^{2/3}). \quad (10)$$

Once H_m has ensured shell formation, mostly of EI type, the variables that become important in modeling configuration mixing are n_ν and z_ν , the number of valence particles in EI spaces of degeneracy D_ν and D_π (see Fig. 1). For the light nuclei these model spaces are unconventional but not necessarily wrong: ^{12}C can be a good core [13], and the $N, Z=14$ closures are at least as convincing as the $N, Z=20$ ones [8].

Spherical nuclei. H_s and subshell effects. The energies of the spherical nuclei will be mocked by H_s , a linear combination of the four operators $S2, S3, SQ+, SQ-$, listed in the second part of Table I, each affected by a coefficient as given in Eq. (4). As explained in [8], H_s is largely devoted to smooth subshell effects. Since S2 is easily absorbed in H_m , and $SQ+$ is not expected (or found) to be important, we are left with only two terms whose main task is to correct the artificial filling patterns due to the imposed degeneracy of the r orbits (we shall return to this point in Sec. III and in the conclusion). The D^β factors in Table I reflect scaling uncertainties associated to these corrections.

Deformed nuclei. H_d . The energies of permanently deformed ground states will be described by the H_d whose form was not derived in [8]; however, it can be easily shown that it must be similar to that of H_s , although the underlying physics is different. The argument is that the onset of deformation is associated with the interruption of normal spherical filling by the promotion of JU_π protons and JU_ν neutrons to configurations of the next HO shell. Nilsson diagrams indicate that $JU_\pi=JU_\nu=JU=4$. The intruders bring a loss of monopole and a gain of quadrupole energy represented by the constant $D0$ (the number 16 in Table I is an arbitrary factor). The deformation energy of the particles in the lower orbits is simulated by quadrupole terms $QQ+$ and $QQ-$, corresponding to the filling of equidistant Nilsson orbits, and $D3$ is in charge of the balance of monopole effects. Scaling is such that deformation energies have the standard $A^{1/3}$ behavior.

TABLE II. Parameters of the $28p$ and $28p^*$ fits— $\mathcal{A} \Rightarrow FM + (28p)$ or $A^{4/3} (28p^*)$ — V_p and V_c given in Table III. The numerical values correspond to binding energies in MeV.

\hat{I}	\mathcal{A}	$PM+$	$4T(T+1)$	$FS+$	$FC+$	$S3$	$D0$	$QQ-$	$PS+$	$PS-$	$FS-$	$D3$	$SQ-$	$QQ+$
$\Gamma 28$	9.55	-0.77	-37.23	6.03	-11.18	0.47	-38.1	25.5	-0.9	-0.13	1.4	-0.9	0.35	4.6
$\rho(\Gamma)28$	0.89	1.3	1.38	4.55	5.11	4.75	4.81	4.09	5.24	5.03	4.21	0	4.47	0
$\Gamma 28^*$	16.73	-0.78	-33.35	6.05	-18.04	0.42	-39.8	13.6	-1.2	-0.16	1.7	0.3	0.16	3.3
$\rho(\Gamma)28^*$	1.44	4.87	1.45	5.39	4.13	4.34	4.79	2.75	6.09	5.30	4.24	0	4.35	0

The fitting procedure and the spherical-deformed boundaries. Energies taken to be positive are given by the expectation values

$$E(N,Z) = \langle H_m \rangle + \langle H_s \rangle (1 - \delta_d) + \langle H_d \rangle \delta_d \\ = \max(\langle H_m \rangle + \langle H_s \rangle, \langle H_m \rangle + \langle H_d \rangle). \quad (11)$$

The lowest possible orbits are filled for spherical nuclei ($\delta d = 0$), while for deformed ones ($\delta d = 1$), JU particles are promoted to orbits j . The calculations are conducted by initializing δd , fitting $E(N,Z)$ in the first equality of Eq. (11) to the 1751 mass values for $N, Z \geq 8$ in the latest compilation [1], then resetting δd through the second part of Eq. (11) and iterating until convergence. Deformed states are only allowed in the regions where neutrons and protons fill different orbits, i.e., above $A \approx 100$. Below, the onset of deformation is not sharp, pairing effects are stronger, and a specific treatment would be called for.

It has already been mentioned that only a particular combination of the master terms was favored, and that the $S2$, $SQ+$, PCA , and PCT contributions would be omitted. In addition, we keep only one XY term and omit the ρ factors in $D3$ and $QQ+$ (the less significant of all the included operators). This leaves us with 28 parameters, shown in Table II. This fit, $28p$, yields an rms error of 375 keV. In the $28p^*$ fit, $\widehat{FM+}$ is replaced by $A^{4/3}$, leading to an rms error of 485 keV. The interest of comparing $28p$ and $28p^*$ will become clear below.

The notation for the operators is $XY \pm = XYA \pm XYT$ and we have preset $JU = 4$, $\alpha = \beta = 1/2$.

It is clear that the ρ ratios fall in two broad categories: for the master terms they are close to unity, and for all others they bunch in the interval 4.5 ± 1 . According to Eq. (4), it means that the corresponding contributions change sign at $\rho \approx A^{1/3}$, i.e., $A \approx 100$, the region where the j orbits can start filling before the r ones are full. This is a clear indication that parametrization (4) acts in a way unrelated to the derivation above, and that all contributions—in addition to doing what they were designed for—are busy simulating subshell effects. Setting $\rho = 0$ is in general of little consequence, except for $S3$, which entails a loss of 300 keV, and to a lesser extent $QQ-$ (loss of 150 keV); and it is possible to obtain fits with rms errors of some 600 keV, with only a dozen parameters.

Some elements of evaluation are given next.

Radii. The radius extracted from V_c , $r \approx 1.235R_c$, is close to the fitted $r \approx 1.225R_c$ [7]. The use of R_c rather than $A^{1/3}$ leads to a gain of 34 keV.

Deformed nuclei. The number of deformed nuclei is 396 for $28p$ and 393 for $28p^*$, with rms errors of 254 and 313 keV respectively. The sharp transitions (e.g., at $N = 89, 90$) are accurately reproduced.

Extrapolation properties. When fitted to the 1503 nuclei in the 1983 compilation, $28p$ yields the rms error of 357 keV. When the same parameter are used on the 248 new nuclei in the 1993 tables the rms error is 470 keV, which amounts to good predictive power by present standards. The increase in error is due only to spherical nuclei, and we have found that discrepancies exceeding 700 keV are almost invariably associated with subshell effects that are important only in spherical regions. Progress in this matter can be expected through a more sophisticated treatment of the S operators.

When it comes to systematic behavior, which includes many spherical nuclei and all the deformed ones (insensitive to subshell details), the fits do very well as emphasized by another test: when $28p$ in Table II is used on the 2542 entries (i.e., including systematic trends) of the 1993 tables the rms error is almost unchanged (407 keV).

The $28p$ and $28p^*$ entries in Table III are the asymptotic contributions, given by Eq. (10) for $FM+$ and $PM+$, plus the Coulomb and pairing terms. Under $6p$ we have the results of a direct fit to the data by varying these six parameters, which can be identified to the classical liquid drop (LD) ones by expanding the R and R^2 denominators (rms error of the $6p$ fit: 2499 keV).

The agreement between $28p$, $28p^*$, and $6p$ in Table III is excellent—even spectacular—except for the surface coefficient in $28p$. (Replacing $FM+$ by FMA leads to an intermediate situation with an rms error of 436 keV and a surface coefficient of -14.6 .)

It is apparent that conventional LD parameters as extracted in $6p$ are fully reproduced by $28p^*$, a very good fit by present standards. However, $28p$ is significantly better and provides a strong hint that the surface energy may be smaller than the conventional value.

The rms errors we have obtained may seem good—even impressive—by present standards, but they are still large compared to those obtained in shell model calculations, i.e., some 300 keV in the lightest nuclei and 150 keV around $A = 100$ [9]. The reason is that our treatment of H_m is too crude since we have forced an artificial degeneracy on the r orbits. As explained in Ref. [8], the correct behavior can be simulated to some extent by the H_s and H_d terms—designed to describe configuration mixing—but also capable of coping

TABLE III. Asymptotic forms of the fits compared with a pure LD form ($6p$). $T2$ stands for $4T(T+1)$. Values in MeV.

	$A^{4/3}/R$	$A^{4/3}/R^2$	$T2/A^{2/3}R$	$T2/A^{2/3}R^2$	V_p	V_c
$28p$	15.07	-12.79	-33.88	48.51	5.18	0.699
$28p^*$	15.39	-17.54	-33.64	49.81	5.15	0.699
$6p$	15.42	-17.56	-33.65	50.91	5.18	0.699

with “monopole drift,” i.e., the smooth part of subshell effects.

A more refined treatment of the S_p operators in H_m will eliminate the large ρ ratios, which are physical—in the sense that they represent a real effect—but mask the true contribution of a given term, and introduce unnecessary phenomenology in the formulation.

It should be clear from these remarks that the fit(s) we

have proposed are only exploratory. There are grounds to expect much better ones.

It takes only seconds to generate a mass table. The program is available from dufloj@frcpn11.in2p3.fr.

We would like to thank G. Audi, G.E. Brown, E. Caurier, T. von Egidy, B. Jonson, P. Möller, H. Niefnecker, M. Pearson, A. Poves, P. Quentin, A. Sobicewsky, F.K. Thielemann, F. Tondeur, and N. Zeldes for useful exchanges.

-
- [1] G. Audi and A.H. Wapstra, Nucl. Phys. **A565**, 1 (1993).
 - [2] G.T. Garvey and I. Kelson, Phys. Rev. Lett. **16**, 197 (1966).
 - [3] S. Liran and N. Zeldes, At. Data Nucl. Data Tables **17**, 431 (1976).
 - [4] J. Jänecke and P. Masson, At. Data Nucl. Data Tables **39**, 265 (1988).
 - [5] P. Möller, J.R. Nix, W.D. Myers, and W.J. Swiatecki, At. Data Nucl. Data Tables, **59**, 185 (1995).
 - [6] Y. Aboussir, J.M. Pearson, A.K. Dutta, and F. Tondeur, Nucl. Phys. **A549**, 155 (1992).
 - [7] J. Duflo, Nucl. Phys. **A576**, 29 (1994).
 - [8] A.P. Zuker, Nucl. Phys. **A576**, 65 (1994).
 - [9] A. Abzouzi, E. Caurier, and A.P. Zuker, Phys. Rev. Lett. **66**, 1134 (1991).
 - [10] A. Bohr and B. Mottelson, *Nuclear Structure I* (Benjamin, New York, 1964)
 - [11] M. Dufour and A.P. Zuker, CRN Report No. 93-29 (1993).
 - [12] W.W. Daehnick, Phys. Rep. **96**, 317 (1983).
 - [13] A.P. Zuker, B. Buck, and J.B. McGrory, Phys. Rev. Lett. **21**, 39 (1968).